Korean J. Chem. Eng., 34(6), 1630-1637 (2017)
DOI: 10.1007/s11814-017-0094-1

pISSN: 0256-1115
eISSN: 1975-7220

Computational fluid dynamics study on the anode feed solid polymer electrolyte water electrolysis

Shuguo Qu†, Guanghui Chen, Jihai Duan, Weiwen Wang, and Jianlong Li

College of Chemical Engineering, Qingdao University of Science & Technology, Qingdao, 266042, Shandong, China
(*Received 22 September 2016 • accepted 1 April 2017*)

Abstract−A steady-state two-dimensional model for the anode feed solid polymer electrolyte water electrolysis (SPEWE) is proposed in this paper. Finite element procedure was employed to calculate the multicomponent transfer model coupled with fluid flow in flow channels and gas diffusion layers and electrochemical kinetics in catalyst reactive surface. The performance of the anode feed SPEWE predicted by this model was compared with the published experimental results and reasonable agreement was reached. The results show that oxygen mass fraction increases because of the water oxidation when water flows from the import to the export on the anode side. On the cathode side, hydrogen mass fraction varies little since hydrogen and water mix well. The flux of water across the electrolyte increased almost linearly with the increase of the applied current density. Since the ohmic overpotential loss increasing as the solid polymer electrolytes' thickness increasing, the performance of the anode feed SPEWE with Nafion 112, 115, 117 decreases at the same applied current density.

Keywords: Computational Fluid Dynamics, Anode Feed Solid Polymer Electrolyte Water Electrolysis, Finite Element Method

INTRODUCTION

The depletion of fossil fuel and protection of the earth's environment have become hot topics and been discussed globally. To overcome those problems, hydrogen energy is put forward to be used as an energy carrier [1]. Hydrogen could be used as a fuel due to its little environmental pollution and as the secondary energy source for power systems, such as fuel cells, stationary power station [2]. Hydrogen is mainly manufactured by steam reforming from natural gas or other fossil fuels, but always accompanied with a high concentration of carbonaceous components such as carbon dioxide and carbon monoxide. High-purity hydrogen (≥99.999% hydrogen) can be prepared through the water electrolysis. Among the technologies for water electrolysis, solid polymer electrolyte water electrolysis (SPEWE) has been developed to produce hydrogen. The main merits of SPEWE over conventional alkaline electrolysis include much better performance, very fast start-up/shut-down rates and much higher purity of the produced hydrogen [3,4]. SPEWE is carried out in an electrolyzer similar to an H_2-O_2 proton exchange membrane fuel cell (PEMFC), but the mechanism is opposite to the mechanism of the PEMFC. When the DC voltage is imposed on the electrolysis system, the water molecules at the anode are broken up into protons and oxygen gas, while electrons are released. Protons go across the electrolyte to the cathode where they are reduced to hydrogen gas by combining electrons from the outer circuit. SPEWE is classified as anode feed system and cathode feed system lying on where water enters the system [5]. When the electrolyzer is used just for generating hydrogen, cathode feed SPEWE could be a better option because the separator which separates oxygen and water is eliminated at the anode and oxygen is ventilated with water. The disadvantage in cathode feed SPEWE is that mass transfer limitations happen and only low current densities can be obtained. In this study, the anode feed SPEWE model was proposed because most of the military and commercial units adopt this form [5]. However, it should be indicated that modelling of cathode feed SPEWE can be achieved with a few changes in water transport phenomenon.

Many experimental studies on SPEWE have been reported [6-9]; however, theoretical analysis has received minimal attention. Millet [2] studied the distribution of electric potential in the Nafion electrolyte through mathematical model. Goldberg [10] developed a hydrodynamic model to study the efficiency of the current collector. Onda et al. [11] proposed a voltage-current relation where the cell voltage is expressed as the sum of anode and cathode overpotentials, resistive overpotential, and Nernst voltage. However, anode and cathode overpotentials are described as a function of the cell current density of the cell and the temperature of the electrolytes by empirical correlations. Electro-osmotic drag coefficient was related to the electrolyte temperature from experiment. Choi [12] used Butler-Volmer kinetics equation to explain the relationship between current and overpotential of SPEWE, but did not consider the water transport in the electrolyte. Awasthi [13] presented a dynamic model of the SPEWE system solved by MATLAB/Simulink to investigate the effect of electrolyzer components and operating conditions on SPEWE's performance. To our best knowledge, the distribution of species and the relationship between water transport and current density has not been reported in the anode feed SPEWE.

†To whom correspondence should be addressed.
E-mail: shuguoqu@163.com

Based on the above reviews, since existing models do not consider the distribution of species (H_2, O_2) and the relationship between water transport and the current density, a comprehensive model for better understanding these phenomena within the anode feed SPEWE is strongly desired. In this paper a two-dimensional, steady state isothermal model for the anode feed SPEWE is proposed to investigate the distribution of hydrogen, oxygen and water in the anode feed SPEWE and the water transport characteristics passing through the electrolyte. The influence of the thickness of the solid polymer electrolytes (such as Nafion 112, Nafion 115 and Nafion 117) on the anode feed SPEWE performance was also explored.

MODEL DEVELOPMENT

In this part, a two-dimensional steady-state isothermal model based on computational fluid dynamics theory for the anode feed SPEWE will be proposed.

1. Model Assumptions

The assumptions of the SPEWE model are as follows:

(1) The catalyst layers at both cathode and anode sides are assumed to be reactive surfaces.

(2) Fluid flow in the anode and cathode channels is laminar due to low Reynolds number.

(3) The gas diffusion layer and the electrolyte are assumed to be isotropous; in addition, electrolyte is imperviable to gas species.

(4) Contact resistance is assumed to be negligible [5].

(6) The SPEWE operates under isotherm conditions.

2. Computational Domain

A drawing of the anode feed SPEWE is shown in Fig. 1. The computational domain includes the anode/cathode flow channels, gas diffusion layers (GDL) and electrolyte regions.

For the anode feed SPEWE, the semi reactions at each electrode and the net water electrolysis reaction are listed as follows:

Anode: $2H_2O \rightarrow 4H^+ + O_2 + 4e^-$

Cathode: $2H^+ + 2e^- \rightarrow H_2$

Total: $2H_2O \rightarrow 2H_2 + O_2$

3. Model Equations

The anode feed SPEWE under isothermal and steady-state conditions is expressed by continuity, species, momentum, electron and proton conservation principles. Therefore, governing equations can be listed as:

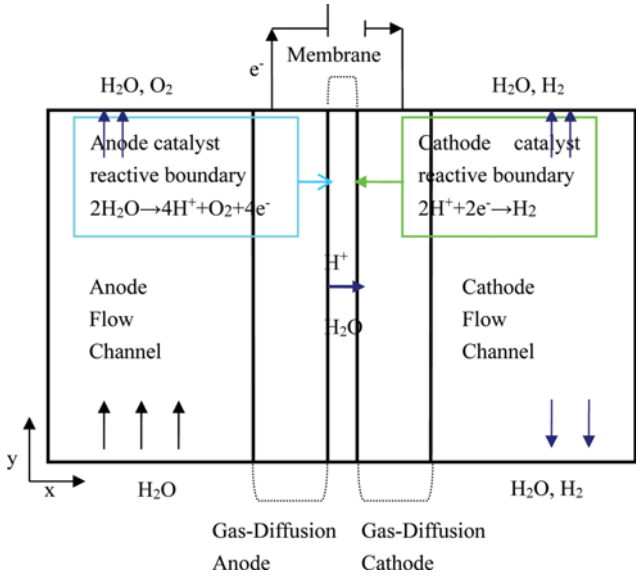

Fig. 1. Schematic illustration of the anode feed SPEWE.

$$\text{Continuity: } \nabla\cdot(\rho \mathrm{u}) = \mathrm{S}_m \tag{1}$$

$$\text{Species: } \nabla\cdot(\mathrm{u}c_k) = \nabla\cdot(\mathrm{D}_k^{eff}\nabla c_k) + \mathrm{S}_k \tag{2}$$

$$\text{Momentum: } \frac{1}{\varepsilon^2}\nabla\cdot(\rho \mathrm{uu}) = -\nabla \mathrm{p} + \nabla\cdot\tau + \mathrm{S}_u \tag{3}$$

$$\text{Electron transport: } -\nabla\cdot(\sigma_s \nabla \Phi_s) = \mathrm{S}_s \tag{4}$$

$$\text{Proton transport: } -\nabla\cdot(\sigma_e \nabla \Phi_e) = \mathrm{S}_e \tag{5}$$

where r is the fluid density, u the fluid velocity vector, S_m the mass source, c_k the molar concentration of species, D_k^{eff} effective diffusion coefficient of species, S_k the source of species, ε the porosity of porous media, p the pressure, τ the shear stress, Su the source term of momentum equation, σ_s the electron conductivity of gas diffusion electrode, S_s the source term of electron, σ_e the proton conductivity of membrane, S_e the source term of proton.

Table 1. Source terms for governing equations in various regions of the anode feed SPEWE

	GDL	Anode reactive surfaces	Cathode reactive surfaces	Membrane
Mass	$S_m=0$	$S_m=M_{O_2}S_{O_2}+M_{H_2O}S_W^a$	$S_m=M_{H_2}S_{H_2}+M_{H_2O}S_W^c$	$S_m=0$
Momentum	$S_u=-\frac{\mu}{K_p}\vec{u}$	$S_u=-\frac{\mu}{K_p}\vec{u}$	$S_u=-\frac{\mu}{K_p}\vec{u}$	/
Species	$S_{H_2}=0$	$S_{H_2}=0$	$S_{H_2}=\frac{i_c}{2F}M_{H_2}$	$S_{H_2}=0$
	$S_{O_2}=0$	$S_{O_2}=\frac{i_a}{4F}M_{O_2}$	$S_{O_2}=0$	$S_{O_2}=0$
	$S_{H_2O}=0$	$S_{H_2O}^a=-(2\alpha+1)\frac{i_a}{2F}M_{H_2O}$	$S_{H_2O}^c=\alpha\frac{i_c}{2F}M_{H_2O}$	$S_{H_2O}=\frac{n_d\cdot I(x,y)}{F}+D_w\cdot\nabla c_w$
Electron	/	$S_s=-i_a$	$S_s=-i_c$	/
Proton	/	$S_e=i_a$	$S_e=-i_c$	/

Table 1 summarizes source terms in above-mentioned governing equations in each sub-domain of the anode feed SPEWE. In gas flow channels, the porosity ε is equal to unity, and Eq. (3) turns into the conventional form of the momentum conservation equation. As for the GDL, S_u is the source term in momentum conservation equation, symbolizing Darcy's drag force. As for the catalyst reactive boundary, the Butler-Volmer kinetic equation [14] is applied to gain the source term of Eqs. (4)-(5):

Anode catalyst reactive boundary:

$$i_a = a i_{0,a}\left(\frac{c_{H_2}}{c_{H_2,ref}}\right)^{1/2}\left(\exp\left(\frac{\partial_a^a F}{RT}\eta_a\right) - \exp\left(\frac{\partial_a^c F}{RT}\eta_a\right)\right) \quad (6)$$

Cathode catalyst reactive boundary:

$$i_c = a i_{0,c}\left(\frac{c_{O_2}}{c_{O_2,ref}}\right)\left(\exp\left(\frac{\partial_c^a F}{RT}\eta_c\right) - \exp\left(\frac{\partial_c^c F}{RT}\eta_c\right)\right) \quad (7)$$

where ∂_a^a, ∂_a^c, are anodic charge transfer coefficient, ∂_c^a, ∂_c^c cathodic charge transfer coefficient, η_a anodic local activation overpotential, η_c cathodic local activation overpotential.

The overall cell potential contains the open circuit voltage, ohmic overpotentials and local activation overpotentials. It can be expressed as [14,15]:

$$V_{cell} = E_{OCV} + \eta_{act} + \eta_{ohm} \quad (8)$$

where E_{OCV} is the open circuit voltage, η_{act} activation polarization (including η_a and η_c), η_{ohm} ohmic polarization. The open circuit voltage is described by Nernst equation [16] as:

$$E_{OCV} = 1.229 - 8.5\times10^{-4}(T - 298.15) + 4.308\times10^{-5}T(\ln(P_{H_2}^*) + 0.5\ln(P_{O_2}^*)) \quad (9)$$

The ohmic overpotential can be written as

$$\eta_{ohm} = IR_{cell} \quad (10)$$

The ohmic resistance, R_{cell} of the SPEWE is the resistance of the proton (H^+) flow in the electrolyte, since the contact resistance between any two parts in the SPEWE is assumed to be negligible, and the resistance of the electrodes and plates is very low compared to the resistance of the electrolyte [17]; only the resistance provided by the proton (H^+) flow in the electrolyte was considered. That electrolyte resistance lies on electrolyte proton conductivity and thickness, and can be shown as:

$$R_{mem} = \frac{t_m}{\sigma_m} \quad (11)$$

where σ_m is the proton conductivity of the electrolyte, t_m electrolyte thickness.

4. Boundary Conditions

4-1. Import and Export of Flow Channels

Only water is fed to the anode of the SPEWE; water flow rate and mass fraction are needed at the import of the anode. For export of anode and cathode flow channels, the boundary conditions for species are defined as convective flux. This guarantees that all the mass transfer through exports is dominated by convection. At the export of anode/cathode flow channels, pressure is set as 1 atm.

4-2. Catalyst Reactive Boundaries

Flux boundary conditions are applied for all the conservation equations at the interface between the gas diffusion layer and the electrolyte which is named catalyst reactive boundary. The boundary conditions are expressed as:

$$N_{O_2} = \frac{i_a}{4F}M_{O_2} \quad (12)$$

$$N_{H_2O}^a = -(2\alpha+1)\frac{i_a}{2F}M_{H_2O} \quad (13)$$

$$N_{H_2} = \frac{i_c}{2F}M_{H_2} \quad (14)$$

$$N_{H_2O}^c = \alpha\frac{i_c}{2F}M_{H_2O} \quad (15)$$

where α represents the whole water dragged from the anode to cathode. It is described as follows:

$$\alpha = n_d - \frac{F}{I}D_w\frac{c_{w,c} - c_{w,a}}{\tau_m} \quad (16)$$

where n_d is water electro-osmotic drag coefficient in the electrolyte, which hinges on the electrolyte water content (λ). In accordance with Zawodzinkski et al. [18], n_d is described as:

$$\begin{aligned} n_d &= 0.2\lambda && \lambda<5 \\ n_d &= 1 && 5\le\lambda\le14 \\ n_d &= 0.1875\lambda - 1.625 && \lambda>14 \end{aligned} \quad (17)$$

The water diffusion coefficient of the electrolyte in Eq. (16) is related to the electrolyte water content and the temperature of the SPEWE, and can be expressed by Motupally et al. [19] as follows:

$$\begin{aligned} D_w &= 3.1\times10^{-7}\lambda[\exp(0.28\lambda) - 1]\exp\left(-\frac{2346}{T}\right) && \lambda\le3 \\ D_w &= 4.17\times10^{-8}\lambda[1 + 161\exp(-\lambda)]\exp\left(-\frac{2346}{T}\right) && \lambda>3 \end{aligned} \quad (18)$$

The mass flux of water at the catalyst reactive boundary equals the electrolyte water flux. The total mass balance of water at anode catalyst reactive boundary is gained by coupling the momentum conservation equation with the flowing expression as:

$$n\cdot u = \left(-\frac{i_a}{4}M_{O_2} - \frac{i_a}{F}M_{H_2O}(\alpha + 0.05)\right)/\rho \quad (19)$$

And the momentum flux at the cathode catalyst reactive boundary is described as:

$$n\cdot u = \frac{1}{2}\left(\frac{i_c}{F}M_{H_2} - \frac{i_c}{F}M_{H_2O}\alpha\right)/\rho \quad (20)$$

The bottoms and tops of the GDL and electrolyte and the sides of the anode/cathode channel are solid boundaries with zero flux of gas passing through them.

The water flux related to the electro-osmotic drag serves as a sink term at the anode catalyst reactive boundary and as a source term at the cathode catalyst reactive boundary. By containing the water flux consumed in the anode electrochemical reaction, the diffusive flux of water at the anode and cathode catalyst reactive boundary from the mass balance can be gained as:

$$J_{w,a} = -\gamma(c_w - c_w^a) - \left(n_d + \frac{1}{2}\right)\frac{I}{F} \quad (21)$$

$$J_{w,c} = -\gamma(c_w - c_w^c) + n_d\frac{I}{F} \quad (22)$$

where, the equilibrium sorption values, c_w^a and c_w^c, are the water concentrations in the body area at the anode and cathode side, c_w the surface water concentration on the electrolyte-side, which lies on the water activity at the respective boundary by Henry's Law, and γ the proportionality constant, meaning the water mass transfer coefficient. In Eqs. (21) and (22), the local water concentration equilibrium value is dependent on the local electrolyte water content λ as follows:

$$c_w^{a,c} = \lambda\frac{\rho_{mem}}{EW_m} \quad (23)$$

The experimental correlation [20] between the electrolyte water content and the water vapor activity (a_k) is applied to compute the electrolyte water content at the catalyst reactive boundary as:

$$\begin{aligned}&\lambda = 0.043 + 17.81a_k - 39.85a_k^2 + 36.0a_k^3;\ 0 < a_k \le 1\\ &\lambda = 14 + 1.4(a_k - 1);\ 1 \le a_k \le 3\\ &\lambda = 16.8;\ a_k \ge 3\end{aligned} \quad (24)$$

The water activity (a_k) in the vapor phase is

$$a_k = \frac{x_{H_2O}P(x,y)}{P_{H_2O}^{sat}} \quad (25)$$

where $P_{H_2O}^{sat}$ is the water saturated vapor pressure of water, and could be calculated using Eq. (26) like [21]:

$$\begin{aligned}\lg P_w^{sat} = &-2.1794 + 0.02953(T - 273.15)\\ &- 9.1837\times10^{-5}(T - 273.15)^2\\ &+ 1.4454\times10^{-7}(T - 273.15)^3\end{aligned} \quad (26)$$

Zawodzinski et al. [22] have measured the electrolyte water content λ of Nafion membranes contacting pure water as 22 and 17 at 30 and 80 °C, respectively. The λ was assumed to be varied linearly between 30 and 80 °C as the following relationship:

$$\lambda = 52.3 - 0.1T \quad (27)$$

Since the anode contacts pure water, $\lambda_a = \lambda$.

5. Solution Technique

The stationary conservation equations of the anode feed SPEWE model are discretized by the finite element procedure and solved by *Comsol Multiphysics 3.5a* software. To achieve the mesh size independence for the numerical solutions, stringent numerical tests were conducted. The mesh size independence test was performed on five mesh size systems. The results of the SPEWE cell potential computed by the model under different mesh size systems when the anode feed SPEWE current density is 0.85 A cm^{-2} are summarized in Table 2. Considering both accuracy and economics the mesh size of 2220 elements was chosen for the present research. Since the iteration process uses much higher computer memory, Femlab software was operated on Dell Precision Workstation (T5810, Intel Xeon E5-1620 V3, 3.5 GHz, 8 GB DDR4). Operating conditions, physical parameters and geometries of the anode feed SPEWE are listed in Table 3.

Table 2. Mesh size independence test

Mesh size	Cell potential (V)
550	1.8307
1110	1.8316
2220	1.8326
3330	1.8330
4440	1.8338

Table 3. Geometries, physical parameters and operating conditions

Parameter	Symbol	Value
Channel length	L_{ch}	20 mm
Channel width	W_{ch}	0.5 mm
Gas diffusion layer thickness	t_{gdl}	200 μm
Membrane thickness (Nafion 112)	t_m	50 μm [23]
Membrane thickness (Nafion 115)	t_m	127 μm [23]
Membrane thickness (Nafion 117)	t_m	177.8 μm [23]
Porosity of anode/cathode gas diffusion layers	ε_{gdl}	0.6 [24]
Anode exchange current density	$i_{a,0}$	0.01 A·m^{-2}
Cathode exchange current density	$i_{c,0}$	100 A·m^{-2}
Permeability of anode/cathode gas diffusion layers	k	1.76×10^{-11} m^2 [25]
Dry membrane density	ρ_{dry}	1980 kg·m^{-3} [26]
Equivalent weight of electrolyte in membrane	EW	1.1 kg·mol^{-1} [26]
Faraday constant	F	96487 C·mol^{-1}
Universal constant	R	8.314 J·mol^{-1}·K^{-1}
Cell temperature	T	328 K
Pressure at the inlet of anode gas channel	$P_{in,a}$	1 atm
Pressure at the inlet of cathode gas channel	$P_{in,c}$	1 atm
Mass transfer coefficient for water	γ	1.14×10^{-4} m·s^{-1}
Membrane conductivity	σ_m	14 S·m^{-1} [27]

RESULTS AND DISCUSSION

In this section, first, the polarization curve of the anode feed SPEWE predicted by the model is validated by the experimental measurement results from literature. Second, the flow behavior and distribution of species in the anode feed SPEWE are presented. Then the relationship between water flux across the electrolyte from anode to cathode and the applied current density is described. Finally, the effect of the thickness of the electrolyte on the performance of the anode feed SPEWE is investigated.

1. Model Validation

To validate the numerical model proposed in this paper, comparisons were made with the experimental data for a single cell operated at 328 K from Millet [2] in Fig. 2. From Fig. 2, the calculated polarization curve of the anode feed SPEWE is consistent with experimental results.

The power supply due to the anode, cathode and ohmic overpotentials are plotted in Fig. 3. The minimum power supply in this figure is the required power supply for overcoming the equilibrium open circuit potential. From Fig. 3, through comparison, anode overpotential is mainly responsible for the voltage rise.

2. Flow Behavior and Distribution of Species in the Anode Feed SPEWE

Fig. 4 describes the velocity distribution in flow channels and

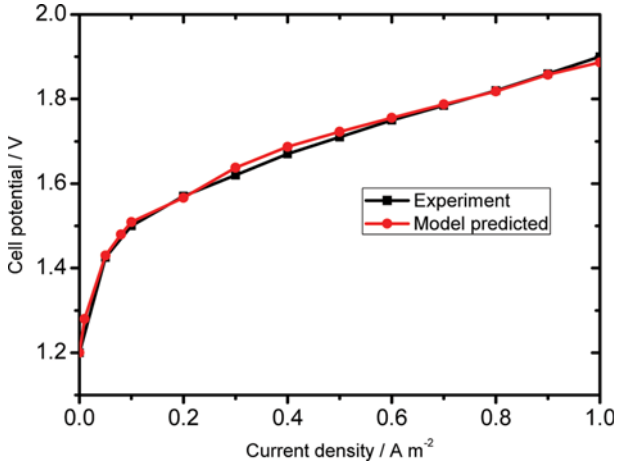

Fig. 2. Comparison of the model predicted and experiment measured cell polarization curves.

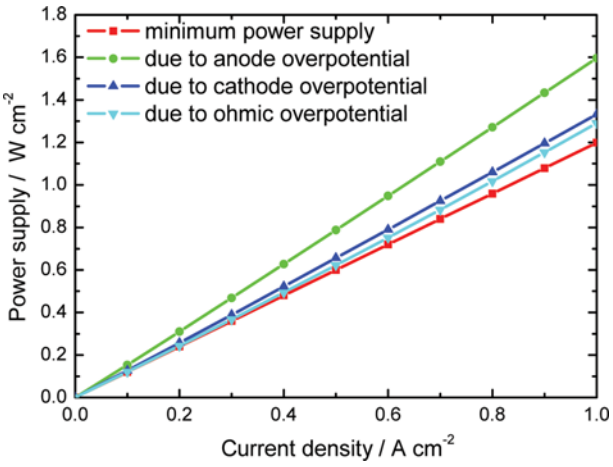

Fig. 3. Required power supply for the anode feed SPEWE due to overpotentials.

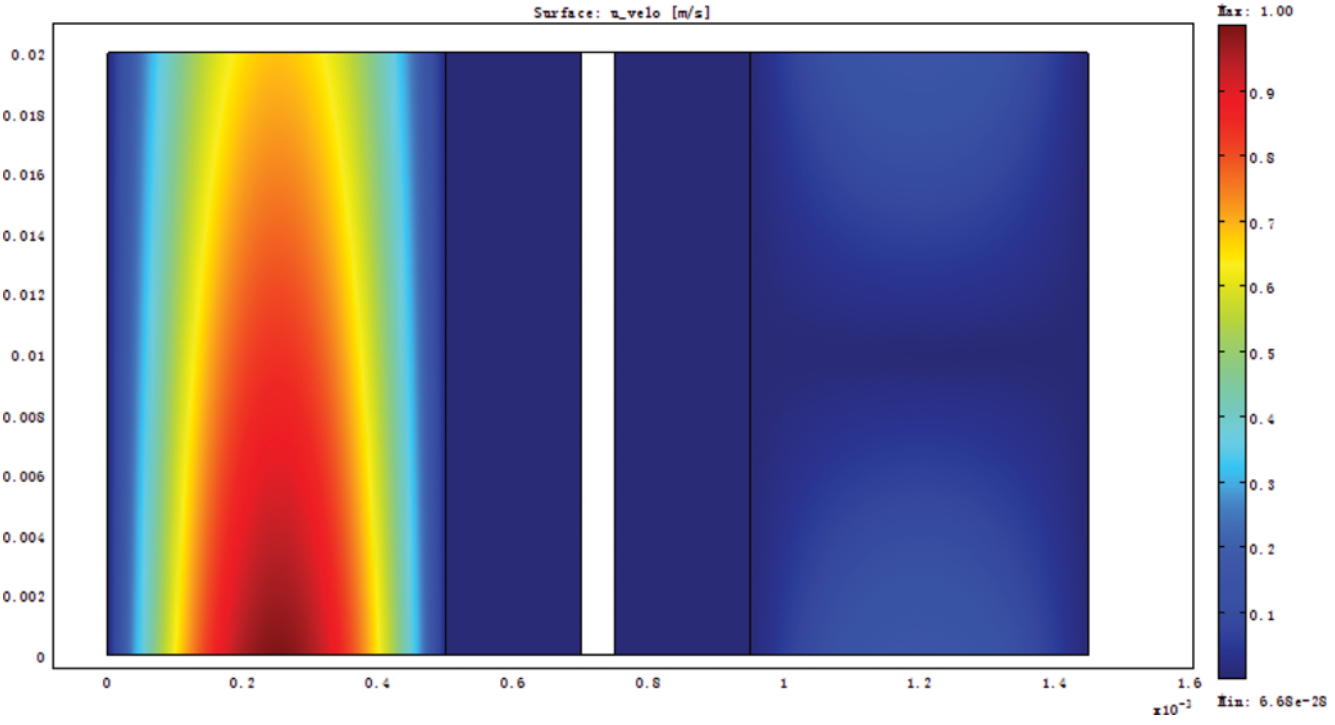

Fig. 4. Surface plot of velocity profile for flow in anode and cathode for a 20 mm long SPEWE.

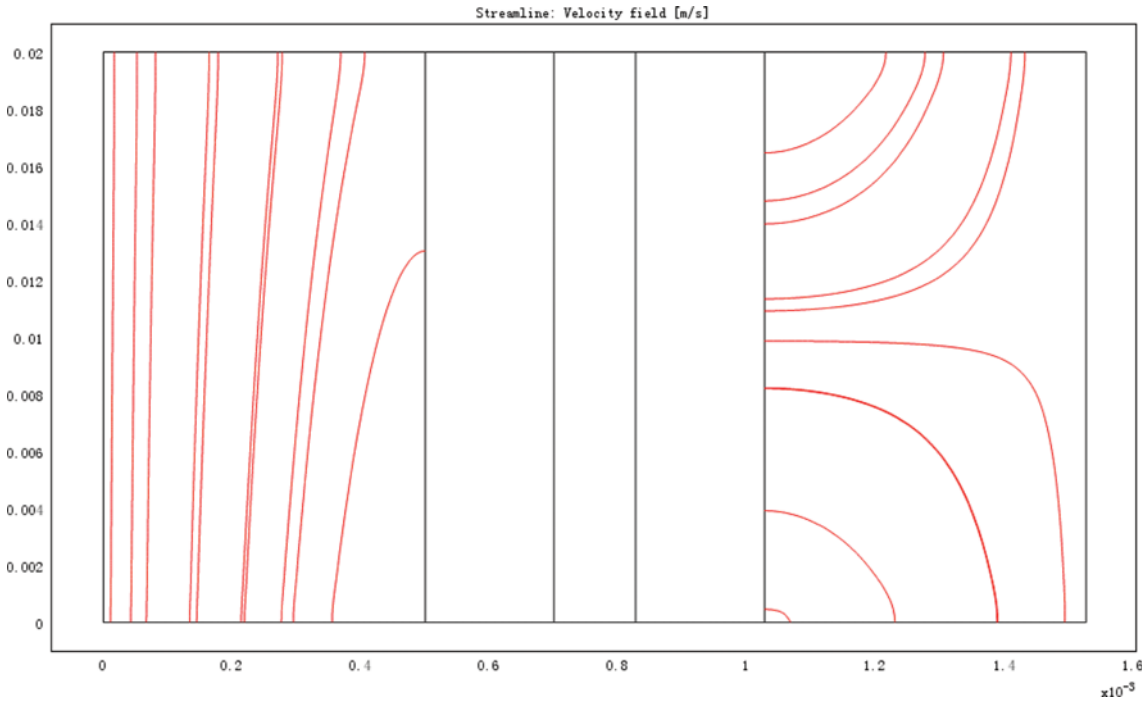

Fig. 5. Computed streamlines for flow in the channels.

porous anode and cathode in the anode feed SPEWE. Since water is only supplied to the anode channel from the bottom and flows upward, the velocity in this domain is higher than other zones in the electrolyzer. At cathode channel, there is only outport, velocity in this domain depends on the produced hydrogen and transported water from anode. The velocity vectors shown in Fig. 4 represent the direction of flow, and the length of vector represents the velocity magnitude. The smaller velocity vectors in the electrodes compared to those in the flow channel indicate a low velocity region since the electrodes are porous media where diffusion dominates the mass transport instead of convection. From the streamlines showed in Fig. 5, it is more evident that velocity vector in cathode channel is outward.

As known, current voltage curves can reveal the cell performance easily, but it is very hard to gain the distribution of species and water content data in the electrolyte experimentally. The calculated distributions of species are shown in Figs. 6, 7, and 8. Fig. 6 shows the oxygen mass fraction distribution on the anode side. As water flows from the import to the outport in the anode side of the SPEWE, the oxygen mass fraction augments. This is due to the influence of the water oxidation. The distribution of hydrogen mass fraction at the cathode side is displayed in Fig. 7. Since there

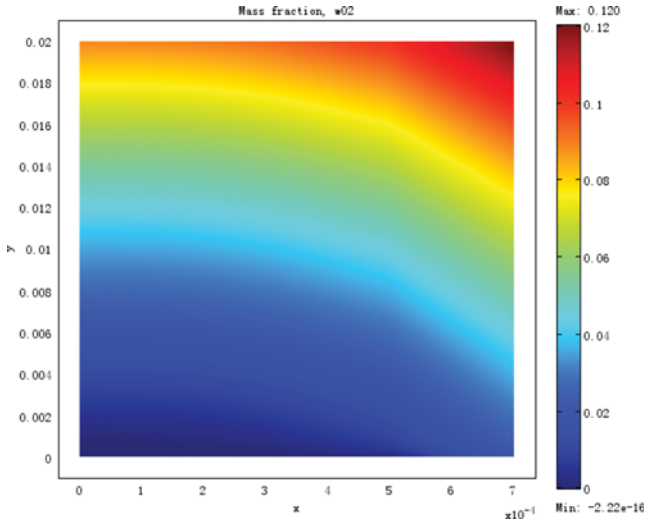

Fig. 6. Surface plot of oxygen mass fraction in anode at the current density of 0.85 A·cm^{-2}.

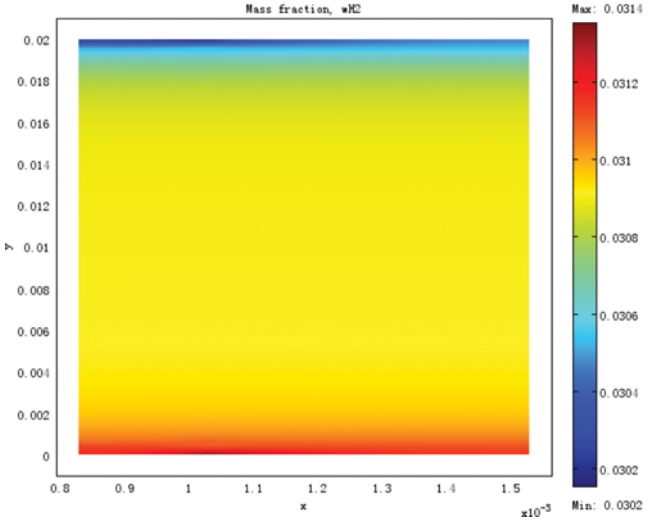

Fig. 7. Surface plot of hydrogen mass fraction in cathode at the current density of 0.85 A·cm^{-2}.

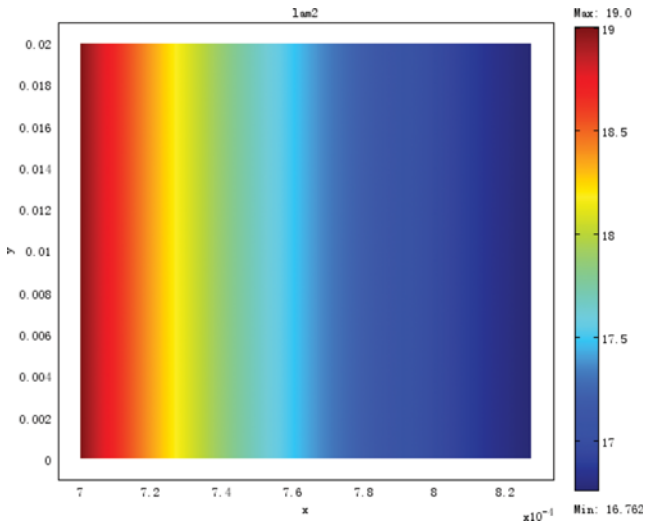

Fig. 8. Surface plot of water content in the membrane at the current density of 0.85 A·cm^{-2}.

is no material entering the cathode of the SPEWE from the inlet of the cathode channel, the produced hydrogen and water from anode mix well and the cathode can be regarded as continuous stirred tank reactor (CSTR). The electrolyte water content is shown in Fig. 8. The membrane interface on the anode side has a specified water content of λ=19, which is calculated from Eq. (27) for the electrolyte in contact with liquid water at 333 K. Since anode feed is adopted, the anode/membrane interface water content is 19. In the electrolyte, water is transferred from anode to cathode due to electro-osmotic and diffusion. So, the electrolyte water content decreases from the anode side to the cathode side.

3. The Influence of Current Density on the Water Flux through the Electrolyte

To estimate the amount of water transported through the electrolyte from the anode to the cathode, the water flux in the x direction was calculated as follows:

$$M_w = \frac{n_d \cdot I}{F} + \frac{\rho_M}{EW_M t_m}\int_{\lambda_c}^{\lambda_a} D_w d\lambda \quad (28)$$

The first term on the right side of Eq. (28) is the water flux due to electro-osmotic drag. The second term is the water diffusion flux. The calculated water flux *vs.* the applied current density was described in Fig. 9. As can be seen in this figure, the water flux increased almost linearly with the increased current density. This means that the water flux due to the diffusion flux only occupies a small portion. So, the electro-osmotic drag coefficient could be gained by the slope of the curve. From Fig. 9, the electro-osmotic drag coefficient of the electrolyte is 2.0.

4. The Influence of Electrolyte Thickness on the Performance of the Anode Feed SPEWE

To account for the influence of electrolyte thickness on the performance of the anode feed SPEWE, three kinds of electrolytes (Nafion 112, 115 and 117) are adopted in this paper. Studies [28] have shown that Nafion 115 and 117 have almost analogous microstructures, but the crystalline component of the polytetrafluoroethylene backbone of Nafion 112 is different from that of Nafion 115 and 117. Hence, Nafion 112 has different electrolyte characters from Nafion 115 and 117, for example, the water diffusion coefficient, permeability, etc. For simplicity, it is assumed that Nafion electrolytes have identical physical characters except thickness in this paper. The thickness of a dry Nafion 112, 115, and 117 electrolyte is 50.8 μm, 127 μm, and 177.8 μm, respectively [23]. From a physical point of view, the ohmic overpotential loss is proportional to the resistor length and inverse ratio on the electrical conductivity. The conductivity of Nafion 112, 115, and 117 electrolyte are supposed to be equal, namely 14 S·m^{-1}. Therefore, the electrolyte ohmic overpotential loss will only depend on the electrolyte thickness, and the ohmic overpotential loss increasing are in the series of Nafion 112, 115, and 117. To put it another way, the performance of the SPEWE decreases with the similar series. This ultimateness can be proved by polarization curves of the anode feed SPEWE with different electrolytes shown in Fig. 10. From Fig. 10, it can be clearly shown that the performance of the anode feed SPEWE decreases with the increasing of electrolyte thickness, especially at higher current densities. For instance, at the current density of 1 A·cm^{-2}, the cell voltage of the anode feed SPEWE used Nafion 112 electrolyte is 1.76 V, while that of Nafion 115 is 1.82 V,

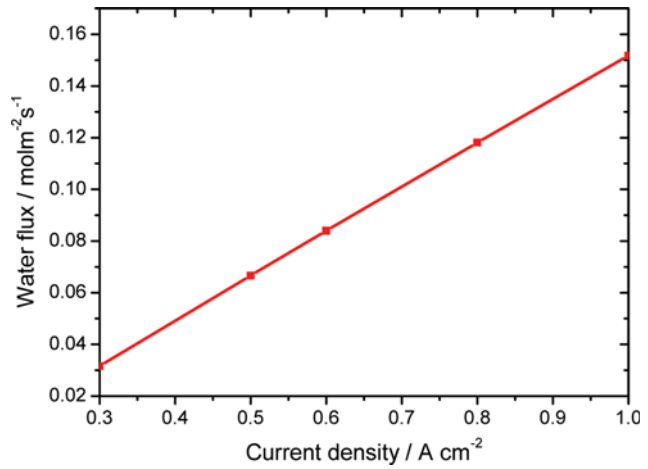

Fig. 9. Water flux across the membrane at different current density.

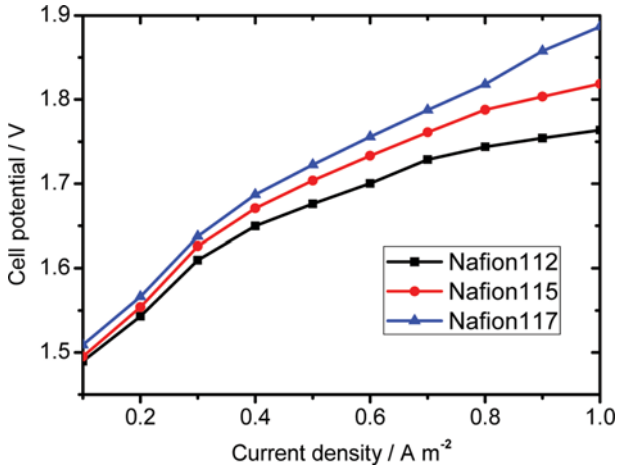

Fig. 10. Performance of the SPEWE with different membranes.

Nafion 117 is 1.89 V.

CONCLUSIONS

A two-dimensional steady-state isothermal model based on computational fluid dynamics theory has been proposed to analyze the performance of the anode feed SPEWE. The predicted polarization curves are consistent with experimental results. This model can analyze the distribution of species and water transport through the electrolyte. As the water flows from the import to the export on the anode side, the oxygen gas mass fraction increases due to the water oxidation. On the cathode side, the hydrogen gas mass fraction has little change because hydrogen gas and water mix well. The flux of water passing through the electrolyte increased almost linearly with the increase of applied current density. As the electrolyte thickness increases, the performance of the anode feed SPEWE with Nafion 112, 115, 117 decreases at the same current density. The proposed model in this paper enables us to reveal the transport phenomenon in the anode feed SPEWE and study the influence of parameter variations such as the electrolyte thickness on the performance of the anode feed SPEWE.

ACKNOWLEDGEMENTS

This work was financially supported by the National Natural Science Foundation of China (No. 21306095).

NOMENCLATURE

a_k : activity of water in stream k, dimensionless
c_w : molar concentration of water in the membrane [mol·m^{-2}]
D : diffusion coefficients [m^2·s^{-1}]
V_{cell} : cell operating potential [V]
E_{OCV} : open-circuit voltage [V]
F : Faraday's constant [96,487 C·mol^{-1}]
I : cell operating current density [A·cm^{-2}]
i_a : anode local current density [A·cm^{-2}]
i_c : cathode local current density [A·cm^{-2}]
$i_{0,a}^{ref}$: anode reference exchange current density [A·m^{-2}]
$i_{0,c}^{ref}$: cathode reference exchange current density [A·m^{-2}]
k_p : hydraulic permeability [m^2]
M_{O_2} : molecular weight of oxygen [kg·mol^{-1}]
M_{H_2} : molecular weight of hydrogen [kg·mol^{-1}]
M_{H_2O} : molecular weight of water [kg·mol^{-1}]
n_d : electro-osmotic drag coefficient
p : pressure [atm]
R : universal gas constant [8.314 J·mol^{-1}·K^{-1}]
T : temperature [K]
t_m : thickness of the electrolyte [m]
u : velocity vector [m·s^{-1}]
w : species mass fraction [dimensionless]
x : species mole fraction [dimensionless]
α : total water drag from the anode to cathode [dimensionless]
γ : mass transfer coefficient for water [m·s^{-1}]
λ : electrolyte water content
ε : porosity of the gas diffusion layer
η : overpotential [V]
μ : viscosity [kg·m^{-1}·s^{-1}]
ρ : density [kg·m^{-3}]
σ_m : membrane electronic conductivity [S·m^{-1}]

REFERENCES

1. M. Carmo, D. L. Fritza, J. Mergela and D. Stolten, *Int. J. Hydrogen Energy*, **38**, 4901 (2013).
2. P. Millet, *Electrochim. Acta*, **39**, 2501 (1994).
3. P. Millet, M. Pineri and R. Durand, *J. Appl. Electrochem.*, **19**, 162 (1989).
4. E. Rasten, G. Hagen and R. Tunold, *Electrochim. Acta*, **48**, 3945 (2003).
5. H. Görgün, *Int. J. Hydrogen Energy*, **31**, 29 (2006).
6. Y. J. Zhang, C. Wang, N. F. Wan, Z. X. Liu and Z. Q. Mao, *Electrochem. Commun.*, **9**, 667 (2007).
7. E. Slavcheva, I. Radev, S. Bliznakov, G. Topalov, P. Andreev and E. Budevski, *Electrochim. Acta*, **52**, 3889 (2007).
8. S. A. Grigoriev, P. Millet and V. N. Fateev, *J. Power. Sources*, **177**, 281 (2008).
9. J. Chattopadhyay, R. Srivastava and P. K. Srivastava, *Korean J. Chem. Eng.*, **30**, 1571 (2013).
10. A. B. Goldberg, L. I. Kheifets, A. G. Vaganov, S. G. Ogryz'ko-Zhukovskaya and A. V. Shabalin, *J. Appl. Electrochem.*, **22,** 1147 (1992).
11. K. Onda, T. Murakami, T. Hikosaka, M. Kobayashi, R. Notu and K. Ito, *J. Electrochem. Soc.*, **149**, A1069 (2002).
12. P. Choi, D. G. Bessarabovb and R. Datta, *Solid State Ionics*, **175**, 535 (2004).
13. A. Awasthi, K. Scott and S. Basu, *Int. J. Hydrogen Energy*, **36**, 14779 (2011).
14. J. O' M. Bockris and S. Srinivasan, Fuel Cells: Their Electrochemistry, McGraw-Hill, New York (1969).
15. T. Thampan, S. Malhotra, J. Zhang and R. Datta, *Catal. Today*, **67**, 15 (2001).
16. A. J. Bard and L. R. Faulkner, Electrochemical Methods, Wiley, New York (1980).
17. X. G. Li, *Principles of fuel cells*, Taylor & Francis (2006).
18. T. A. Zawodzinski, J. Davey, J. Valerio and S. Gottesfeld, *Electrochim. Acta*, **40**, 297 (1995).
19. S. Motupally, A. J. Becker and J. W. Weidner, *J. Electrochem. Soc.*, **147**, 3171 (2000).
20. T. E. Springer, T. A. Zawodzinski and S. Gottesfeld, *J. Electrochem. Soc.*, **138**, 2334 (1991).
21. R. H. Perry and D. W. Green, Perry's Chemical Engineer's Handbook, Seventh Ed. (1997).
22. T. A. Zawodzinski, T. E. Springer, J. Davey, R. Jestel, C. Lopez, J. Valerio and S. Gottesfeld, *J. Electrochem. Soc.*, **140**, 1981 (1993).
23. H. Wu, P. Berg and X. Li, *J. Power. Sources*, **165**, 232 (2007).
24. G. H. Guvelioglu and H. G. Stenger, *J. Power. Sources*, **147**, 95 (2005).
25. T. F. Fuller and J. Newman, *J. Electrochem. Soc.*, **5**, 1218 (1993).
26. H. Meng and C. Y. Wang, *Chem. Eng. Sci.*, **59**, 3331 (2004).
27. K. Scott, W. Taama and J. Cruickshank, *J. Power. Sources*, **65**, 159 (1997).
28. S. Sportsman, D. Way and G. Pez, The 13th annual meeting of the North American Membrane Society, Long Beach, California (2002).